Journal of the Nigerian Association of Mathematical Physics
Volume28, No. 1, (November, 2014), pp 405 – 414

Analysis of Temperature Distribution in Wellbore During Drilling Operation Using Finite Element Method

[1]C.I. Oviawe, [2]L.M. Osite, [3]O.S.Wilkie and [4]I.O. Momodu

[1, 2]Department of Mechanical Engineering, Edo State Institute of Technology and Management, Usen, P.M.B. 1104, Benin City
[3]Department of Petroleum Engineering, Edo State Institute of Technology and Management,Usen.
[4]Department of Computer Science Edo State Institute of Technology and Management,Usen.

Abstract

This paper presents a mathematical modeling of the temperature distribution set up at various cross-section of well bore during drilling operation by the weighted residual finite element method. We present the numerical solution to the one-dimensional differential equation which describes the temperatures exerted on the drilling wellbore. In conducting the analysis, we split the blank into a finite number of elements and apply the Bubnov-Galerkin weighted residual scheme to obtain the weighted integral form, the finite element method was then developed and solved to yield a three-parameter polynomial solution. Using a numerical example, the result showed that the weighted residual finite element method was capable of accurately predicting the temperature distribution in wellbore with fluid having constant properties.

Keywords: Well bore, temperature, Galerkin, drilling, finite element.

Nomenclature

K_f : Formation thermal conductivity (Btu/Ft- ^oF – hour)
ℓ_F : Formation density (1b/gal)
C_F : Formation heat capacity (Btu/1b-^oF)
M: Mass flow rate of drilling fluid (1b/hr)
C_{ft} : Fluid heat capacity (Btu/1b.^oF
r_p : Radius of drill pipe (ft)
U_p : Equivalent heat transfer coefficient across pipe wall (Btu/hr-ft^2-^oF
h : Depth (ft)
T_{Fs} : Surface formation temperature (^oF)
g_{Gx} : Geothermal gradient (^oF/ft)
T_p : Temperature of drill pipe fluid as a function of depth (^oF)

1.0 Introduction

A knowledge of temperature distribution of circulating drilling fluids in wellbore and the surrounding formation is required to calculate the frictional pressure drop and also to predict the transient thermal behvaiour of the well during drilling operation and completion. This, information is useful for correct drilling job design execution and for deciding whether drilling should be stopped or continued. This, inturn reflect in the final costs of the completed well drilled. The determination of the transient temperature is a complex task because there are a number of influence variables that are continuously changing.

A number of studies on drilling fluid temperature profile estimation exist in literature. Arnold [1] determined the temperature variation in a circulating wellbore fluid. Beirute [2] estimated the circulating and shut-in well temperature profile. Garcia et al [3] an estimation of temperatures in geothermal wells during circulation shut-in in presence of loss

Corresponding author:C.I. Oviawe E-mail: iyekowa@yahoo.co.uk, Tel.: +2348055805619 and 08162691127

circulation. Romey [4] evaluated wellbore heat transmission. Raymond [5] evaluated the temperature distribution in circulating drilling fluids. Rommetveit and Bjorkevoll [6] estimated the temperature and pressure effects on drilling fluid Rheology and ECD in vary wells depth. Takahashi et al [7] estimation of formation temperature from inlet and outlet mud temperature while drilling. Traggaser et al [8] a method for calculating circulating temperature. Wooley [9] computed downhole temperature in circulation injection and production wells.
It can be seen from the literature that the potential of the finite element method for obtaining solution temperature distribution problems have not been given attention. In this paper, we present the application of the continuous Galerkin finite element method to the analysis of temperature distribution in wellbore during drilling operation and compare the solution obtained with that of analytical technique.

2.0 Mathematical modeling

$$\alpha\beta\frac{d^2T_p}{dx^2}+\beta\frac{dT_p}{dx}=T_p-T_{Fs}-g_{Gx} \tag{2.1}$$

Where

$$\alpha=\frac{K_F}{\ell_F C_F} \quad and \quad \beta=\frac{MC_{fl}}{2\pi r_p U_p}$$

Equation (2.1) gives the governing differential equation
The associated boundary conditions are given by:

$$T(o)=T_o,\ \frac{dT_p}{dx}=0,\ q(h')=q \tag{2.2}$$

Where q is the heat flux and is given by the expression $\frac{\beta dTp}{dx}$

The following assumptions were made in developing this mathematical model thus:

- Assume constant fluid properties
- Heat generated by viscous forces, friction and changes in potential energy are negligible
- The formation is radially symmetric and infinite with respect to heat flow
- Heat flow within the wellbore is rapid compared to heat flow within the formation
- Assume heat flow within and across the wellbore conduits to be steady state and while heat flow within the formation to be transient

2.1 Materials and Methods

The spatial domain of the wellbore was divided into a number of uniform linear elements with length ΔX . Stiffness matrices were generated for each element using the finite element model to get the temperature at nodal points. The stiffness matrices were assembled by enforcing continuity of the nodal degree of freedom to obtain the global system equations. The Lagrenge quadratic interpolation functions were used to ensure an accurate solution. A numerical analysis was done to compare the finite element results with the exact solution.

2.2 Finite Element Modeling

To determine the temperature distribution in wellbore during drilling operation, we first derive the weak form of the governing differential equation. This we obtained by using the Galerkin weighted residual method. Multiplying the residual of the equation by a weight function (w) and integrating over the domain enclosing an element with respect to X.

$$\int_o^h w\left(\alpha\beta\frac{d^2T_p}{dx^2}+\beta\frac{dTp}{dx}-T_p+T_{Fs}+g_{Gx}\right)dx=0 \tag{2.3}$$

Let $T_F = T_{Fs} + g_{Gx}$ (2.4)

Substituting equation (2.4) into equation (2.3) gives

$$\int^h w\left(\alpha\beta\frac{d^2T_p}{dx^2}+\beta\frac{dT_p}{dx}-T_p+T_F\right)dx=0 \tag{2.5}$$

$$\int^h\left(w\alpha\beta\frac{d^2T_p}{dx^2}+w\beta\frac{dT_p}{dx}-wT_p+wT_F\right)dx=0 \tag{2.6}$$

An examination of equation (2.6) reveals the solution and hence once differentiable with respect to X. Thus the Lagrange quadratic functions of interpolation can be used satisfactorily. Assuming an approximate solution for T_p in the form as follows:

$$T_p \approx T_p^e = \sum_{j=1}^{n} T_p \psi_j^e(x) \qquad (2.7)$$

Where,

ψ_j^e = Lagrange quadratic function of interpolation at the jth node

T_{pj}^e = Temperature at the jth node of the element

Since we are applying the Galerkin weighted residual finite element method in this study, we assume that the weight function is equal to the Lagrange function of interpolation

$$w = \psi_j^e(x) \qquad (2.8)$$

That is,

$$\frac{dwdx}{dx} = \frac{d\psi_j^e}{dx}dx \qquad (2.9)$$

Substituting equation (2.7) and (2.9) into equation (2.6) gives

$$\sum_{j=I}^{n}\int^{h'} \alpha\beta\left(Tp_j^e \frac{d\psi_j^e}{dx}\cdot\frac{d\psi_j^e}{dx} + \beta Tp_j^e \frac{d\psi_j^e}{dx}\right)dx - \psi_j^e\int^{h}\left(T_p + T_f\right)dx = 0 \qquad (2.10)$$

$$\sum_{j=I}^{n}\int^{h'} \alpha\beta\left(\frac{d\psi_j^e}{dx}\cdot Tp_j^e\frac{d\psi_j^e}{dx} + \beta\psi_j^e Tp_j^e\frac{d\psi_j^e}{dx} - \psi_j^e T_{p_j}\psi_j^e\right)dx + \int^{h}\psi_j^e T_F dx - wQ(h') - wQ(o) = 0$$

(2.11)

Equation (2.11) can be translated as:

$$\left[K_{ij}^e\right]\left\{Tp_j^e\right\} + \left[M_{ij}^e\right]\left\{Tp_j^e\right\} = \left\{F_{ij}^e\right\} + \left\{Q_{ij}^e\right\} \qquad (2.12)$$

Equation (2.12) is called the finite element model for the problem.

Where

$\left[K_{ij}^e\right]\left\{Tp_j^e\right\} =$ Characteristic matrix

$\left[M_{ij}^e\right]\left\{Tp_j\right\} =$ Mass matrix

$\left\{F_{ij}^e\right\}$ = Characteristic vector

$\left\{Q_{ij}^e\right\}$ = Boundary vector

Where

$$K_{ij}^e = \int^{h'} \alpha\beta\left(\frac{d\psi_j^e}{dx}\cdot\frac{d\psi_j^e}{dx} + \psi_i^e\psi_j^e\right)dx$$

$$M_{ij}^e = \int^{h'} \beta\psi_i^e\frac{d\psi_j^e}{dx}$$

$$F_{ij}^e = \int^{h'} \psi_i^e T_F dx$$

Q_{ij}^e = denote heat flow into the element at node. Using the Lagrange quadratic interpolation functions

$$\psi_1^e = \left(1 - \frac{x}{h'}\right)\left(1 - \frac{2x}{h'}\right)$$

$$\psi_2^e = \frac{4x}{h'}\left(1 - \frac{2x}{h'}\right)$$

$$\psi_3^e = -\frac{x}{h'}\left(1 - \frac{2x}{h'}\right)$$

To simplify the calculation of the element characteristic and mass matrix for different meshes we generate an expression for the entries of the element characteristic and mass matrix in terms of the depth of each element h'. Thus

$$K_{11}^e = \int_o^{h'} \left(\alpha\beta \frac{d\psi_1^e}{dx}\frac{d\psi_1^e}{dx} + \psi_1^e \psi_1^e \right) dx$$

$$= \frac{7\alpha\beta}{3h'} + \frac{2h'}{15}$$

$$K_{12}^e = \int^{h'} \left(\alpha\beta \frac{d\psi_1^e}{dx}\frac{d\psi_2^e}{dx} + \psi_1^e \psi_2^e \right) dx$$

$$- \frac{8\alpha\beta}{3h'} + \frac{h'}{15}$$

$$K_{13}^e = \int^{h'} \left(\alpha\beta \frac{d\psi_1^e}{dx}\frac{d\psi_3^e}{dx} + \psi_1^e \psi_3^e \right) dx$$

$$= \frac{\alpha\beta}{3h'} - \frac{h'}{30}$$

$$K_{21}^e = \int_o^{h'} \left(\alpha\beta \frac{d\psi_2^e}{dx}\frac{d\psi_1^e}{dx} + \psi_2^e \psi_1^e \right) dx$$

$$= \frac{-8\alpha\beta}{3h'} + \frac{h'}{15}$$

$$K_{22}^e = \int_o^{h'} \left(\alpha\beta \frac{d\psi_2^e}{dx}\frac{d\psi_2^e}{dx} + \psi_2^e \psi_2^e \right) dx$$

$$= \frac{\alpha\beta 16}{3h'} + \frac{16h'}{30}$$

$$K_{23}^e = \int_o^{h'} \left(\alpha\beta \frac{d\psi_2^e}{dx}\frac{d\psi_3^e}{dx} + \psi_2^e \psi_3^e \right) dx$$

$$= -\frac{8\alpha\beta}{3h'} + \frac{h'}{15}$$

Due to symmetry

$$K_{13}^e = -K_{31}^e = \frac{-\alpha\beta}{3h'} + \frac{h'}{30}$$

$$K_{12}^e = -K_{32}^e = \frac{8\alpha\beta}{3h'} - \frac{h'}{15}$$

$$K_{11}^e = K_{33}^e = \frac{-7\alpha\beta}{3h'} - \frac{2h'}{15}$$

For the mass matrix

$$M_{11}^e = \int_o^{h'} \beta\psi_1^e \frac{d\psi_1^e}{dx} = \frac{3\beta}{6}$$

$$M_{12}^e = \int_o^{h'} \beta\psi_1^e \frac{d\psi_2^e}{dx} = \frac{2\beta}{3}$$

$$M_{13}^e = \int_o^{h'} \beta\psi_1^e \frac{d\psi_3^e}{dx} = -\frac{\beta}{6}$$

$$M_{21}^e = \int_o^{h'} \beta\psi_2^e \frac{d\psi_1^e}{dx} = -\frac{2\beta}{3}$$

$$M_{22}^e = \int_o^{h'} \beta\psi_2^e \frac{d\psi_2^e}{dx} = 0$$

$$M_{23}^{e}=\int_{o}^{h'}\beta\psi_{2}^{e}\frac{d\psi_{3}^{e}}{dx}=\frac{2\beta}{3}$$

Due to symmetry

$$M_{33}^{e}=-M_{11}^{e}=\frac{3\beta}{6}$$

$$M_{32}^{e}=-M_{12}^{e}=\frac{4\beta}{6}$$

$$M_{31}^{e}=-M_{13}^{e}=\frac{\beta}{6}$$

Hence for one Lagrange quadratic element will be

$$\left[K_{ij}^{e}\right]=\frac{\alpha\beta}{3h'}\begin{bmatrix}7 & -8 & 1\\ -8 & 16 & -8\\ 1 & -8 & 7\end{bmatrix}+\frac{h'}{30}\begin{bmatrix}4 & 2 & -1\\ 2 & 16 & -8\\ -1 & 2 & 4\end{bmatrix} \quad (2.13)$$

$$\left[M_{ij}^{e}\right]=\frac{\beta}{6}\begin{bmatrix}-3 & 4 & -1\\ -4 & 2 & 4\\ 1 & -4 & 3\end{bmatrix} \quad (2.14)$$

3.0 Numerical example

Use the finite element method to find the temperature distribution in the wellbore during drilling operation. The governing differential equation is given by:

$$\frac{\alpha\beta d^{2}T_{p}}{dx^{2}}+\frac{\beta dT_{p}}{dx}=T_{p}-T_{F}-g_{G}$$

Given:

Well depth (h')=80ft, outer drill pipe radius (r_p) = 0.208ft, Annulus radius (r_a)=0.354ft, circulation rate = 400bbl/hr, Circulation time(hr) = 5hrs, Surface formation temperature (T_{Fs})=60^{oF}, Thermal conductivity (K_f) = 0.3Btu/ft^{-oF-}hr, Specific heat capacity (C_f) = 0.21Btu/b^{-oF}, Density (ℓ_F)=1651b/ft^3, Geothermal gradient (g_G) = 0.020 ^{oF}/ft, α=1.25 and β=0.80, Inlet mud temperature (T_{ps})=120^{oF}

3.1 Solution:

3.11 Quadratic element interpolation solution

We seek the nodal temperature by using quadratic interpolation functions. We computed the quadratic element characteristic matrix and mass matrix by substituting for α, β and h' in equations (2.13) and (2.14). Thus we obtain:

$$\left[K_{ij}^{e}\right]=\begin{bmatrix}2.785 & 1.201 & -0.650\\ 1.201 & 10.940 & 1.201\\ -0.650 & 1.201 & 2.785\end{bmatrix} \quad (3.1)$$

$$\left[M_{ij}^{e}\right]=\begin{bmatrix}-0.399 & 0.532 & -0.133\\ -0.532 & 0 & 0.532\\ 0.133 & -0532 & 0.399\end{bmatrix} \quad (3.2)$$

In order to ensure high accuracy, we used a mesh of four quadratic elements (9 nodes). Dividing the domain into four 1-D quadratic finite elements and the finite elements model over an element is given as:

$$K_{ij}^{e}=\begin{bmatrix}K_{11}^{e} & K_{12}^{e} & K_{13}^{e}\\ K_{21}^{e} & K_{22}^{e} & K_{23}^{e}\\ K_{31}^{e} & K_{32}^{e} & K_{33}^{e}\end{bmatrix} \quad (3.3)$$

$$M_{ij}^{e} = \begin{bmatrix} M_{11}^{e} & M_{12}^{e} & M_{13}^{e} \\ M_{21}^{e} & M_{22}^{e} & M_{23}^{e} \\ M_{31}^{e} & M_{32}^{e} & M_{33}^{e} \end{bmatrix} \tag{3.4}$$

For a mesh of four I-D quadratic elements the assembled equations are:

$$\begin{bmatrix} K_{11}^{1} & K_{21}^{1} & 0 & 0 & 0 & 0 & 0 & 0 & 0 \\ K_{21}^{1} & K_{22}^{1} & K_{23}^{1} & 0 & 0 & 0 & 0 & 0 & 0 \\ K_{31}^{1} & K_{32}^{1} & K_{11}^{1}+K_{33}^{2} & K_{12}^{2} & K_{13}^{2} & 0 & 0 & 0 & 0 \\ 0 & 0 & K_{21}^{2} & K_{22}^{2} & K_{23}^{2} & 0 & 0 & 0 & 0 \\ 0 & 0 & K_{31}^{2} & K_{32}^{2} & K_{11}^{3}+K_{33}^{3} & K_{12}^{3} & K_{13}^{3} & 0 & 0 \\ 0 & 0 & 0 & 0 & K_{21}^{3} & K_{22}^{3} & K_{23}^{3} & 0 & 0 \\ 0 & 0 & 0 & 0 & K_{31}^{3} & K_{32}^{3} & K_{11}^{4}+K_{33}^{3} & K_{12}^{4} & K_{13}^{4} \\ 0 & 0 & 0 & 0 & 0 & 0 & K_{21}^{4} & K_{22}^{4} & K_{23}^{4} \\ 0 & 0 & 0 & 0 & 0 & 0 & K_{31}^{4} & K_{32}^{4} & K_{33}^{4} \end{bmatrix} \begin{bmatrix} Tp_1 \\ Tp_2 \\ Tp_3 \\ Tp_4 \\ Tp_5 \\ Tp_5 \\ Tp_6 \\ Tp_7 \\ Tp_8 \\ Tp_9 \end{bmatrix} +$$

$$\begin{bmatrix} M_{11}^{1} & M_{21}^{1} & 0 & 0 & 0 & 0 & 0 & 0 & 0 \\ M_{21}^{1} & M_{22}^{1} & M_{23}^{1} & 0 & 0 & 0 & 0 & 0 & 0 \\ M_{31}^{1} & M_{32}^{1} & M_{11}^{1}+M_{33}^{2} & M_{12}^{2} & M_{13}^{2} & 0 & 0 & 0 & 0 \\ 0 & 0 & M_{21}^{2} & M_{22}^{2} & M_{23}^{2} & 0 & 0 & 0 & 0 \\ 0 & 0 & M_{31}^{2} & M_{32}^{2} & M_{11}^{3}+M_{33}^{3} & M_{12}^{3} & M_{13}^{3} & 0 & 0 \\ 0 & 0 & 0 & 0 & M_{21}^{3} & M_{22}^{3} & M_{23}^{3} & 0 & 0 \\ 0 & 0 & 0 & 0 & M_{31}^{3} & M_{32}^{3} & M_{11}^{4}+M_{33}^{3} & M_{12}^{4} & M_{13}^{4} \\ 0 & 0 & 0 & 0 & 0 & 0 & M_{21}^{4} & M_{22}^{4} & M_{23}^{4} \\ 0 & 0 & 0 & 0 & 0 & 0 & M_{31}^{4} & M_{32}^{4} & M_{33}^{4} \end{bmatrix} \begin{bmatrix} Tp_1 \\ Tp_2 \\ Tp_3 \\ Tp_4 \\ Tp_5 \\ Tp_5 \\ Tp_6 \\ Tp_7 \\ Tp_8 \\ Tp_9 \end{bmatrix} =$$

$$\begin{bmatrix} F_1^1 \\ F_2^1 \\ F_3^1+F_1^2 \\ F_3^2+F_1^3 \\ F_2^3+F_1^4 \\ F_3^4+F_1^5 \\ F_2^5+F_1^6 \\ F_2^6 \\ F_3^6 \end{bmatrix} + \begin{bmatrix} Q_1^1 \\ Q_2^1 \\ Q_3^1+Q_1^2 \\ Q_3^2+Q_1^3 \\ Q_2^3+Q_1^4 \\ Q_3^4+Q_1^5 \\ Q_2^5+Q_1^6 \\ Q_2^6 \\ Q_3^6 \end{bmatrix} \tag{3.5}$$

For characteristic vector evaluation entries

$$F_{ij}^{e} = \int_{o}^{h'} \psi_j^e T_F \, dx$$

Where $T_F = T_{Fs} + g_G = 60+0.020 = 60.020^{o}F$, $h' = 80\,ft$

$$F_1^e = \int_o^{h'} \psi_j^e T_F \, dx = \int_o^{h'} \left(1-\frac{x}{h'}\right)\left(1-\frac{2x}{h'}\right) T_F \, dx$$

$$= \left[x - \frac{3x^2}{2h'} + \frac{2x^3}{3h^{21}}\right]_o^{h'} T_F \, dx = \frac{h' T_F}{6}$$

$$F_2^e = \int_o^{h'} \psi_2^e T_F \, dx = \int_o^{h'} \frac{4x}{h'}\left(1-\frac{x}{h'}\right) T_F \, dx$$

$$= \left[\frac{2x^2}{h'} - \frac{4x^3}{3h^{21}}\right]_o^{h'} T_F \, dx = \frac{2h' T_F}{3}$$

$$F_3^e = \int_o^{h'} \psi_3^e T_F \, dx = \int_o^{h'} \frac{-x}{h'}\left(1 - \frac{2x}{h'}\right) T_F \, dx$$

$$= \left[\frac{-x^2}{2h'} + \frac{2x^3}{3h^{21}}\right]_o^{h'} T_F \, dx = \frac{h' T_F}{6}$$

$$F^e = \begin{bmatrix} F_1^1 \\ F_2^1 \\ F_3^1 + F_1^2 \\ F_3^2 + F_1^3 \\ F_2^3 + F_1^4 \\ F_3^4 + F_1^5 \\ F_2^5 + F_1^6 \\ F_2^6 \\ F_3^6 \end{bmatrix} = 800.2 \begin{bmatrix} 1 \\ 4 \\ 2 \\ 5 \\ 2 \\ 5 \\ 2 \\ 4 \\ 1 \end{bmatrix} \qquad (3.7)$$

Due to balance of internal influxes, it follows that $Q!_3^1 + Q_1^2 = Q_3^2 + Q_1^3 = Q_3^3 + Q_1^4 = 0$ and $Q_2^4 = Q_2^5 = Q_2^6 = 0$

Substituting the values of equations (3.1), (3.2) and (3.7) into equation (3.5) we obtain:

$$\begin{bmatrix} 2.785 & 1.201 & -0.650 & 0 & 0 & 0 & 0 & 0 & 0 \\ 1.201 & 10.940 & 1.201 & 0 & 0 & 0 & 0 & 0 & 0 \\ -0.650 & 1.201 & 5.570 & 1.201 & -0.650 & 0 & 0 & 0 & 0 \\ 0 & 0 & 1.201 & 10.940 & 1.201 & 0 & 0 & 0 & 0 \\ 0 & 0 & -0.650 & 1.201 & 5.570 & 1.201 & -0.650 & 0 & 0 \\ 0 & 0 & 0 & 0 & 1.201 & 10.940 & 1.201 & 0 & 0 \\ 0 & 0 & 0 & 0 & -0.650 & 1.201 & 5.570 & 1.201 & -0.650 \\ 0 & 0 & 0 & 0 & 0 & 0 & 1.201 & 10.940 & 1.201 \\ 0 & 0 & 0 & 0 & 0 & 0 & -0.650 & 1.201 & 2.785 \end{bmatrix} \begin{bmatrix} Tp_1 \\ Tp_2 \\ Tp_3 \\ Tp_4 \\ Tp_5 \\ Tp_5 \\ Tp_6 \\ Tp_7 \\ Tp_8 \\ Tp_9 \end{bmatrix} +$$

$$\begin{bmatrix} -0.399 & 0.532 & -0.133 & 0 & 0 & 0 & 0 & 0 & 0 \\ -0.532 & 0 & 0.532 & 0 & 0 & 0 & 0 & 0 & 0 \\ 0.133 & -0.532 & 0 & 0.532 & -0.133 & 0 & 0 & 0 & 0 \\ 0 & 0 & -0.532 & 0 & 0.532 & 0 & 0 & 0 & 0 \\ 0 & 0 & 0.133 & -0.532 & 0 & 0.532 & -0.133 & 0 & 0 \\ 0 & 0 & 0 & 0 & -0.532 & 0 & 0.532 & 0 & 0 \\ 0 & 0 & 0 & 0 & 0.133 & -0.532 & 0 & 0.532 & -0.133 \\ 0 & 0 & 0 & 0 & 0 & 0 & -0.532 & 0 & 0.532 \\ 0 & 0 & 0 & 0 & 0 & 0 & 0.133 & -0.532 & 0.399 \end{bmatrix} \begin{bmatrix} Tp_1 \\ Tp_2 \\ Tp_3 \\ Tp_4 \\ Tp_5 \\ Tp_5 \\ Tp_6 \\ Tp_7 \\ Tp_8 \\ Tp_9 \end{bmatrix} =$$

$$800.2 = \begin{bmatrix} 1 \\ 4 \\ 2 \\ 5 \\ 2 \\ 5 \\ 2 \\ 4 \\ 1 \end{bmatrix} + \begin{bmatrix} Q_1 \\ 0 \\ 0 \\ 0 \\ 0 \\ 0 \\ 0 \\ 0 \\ Q_9 \end{bmatrix} \qquad (3.8)$$

We apply row sum lumping technique and the mass matrix in equation (3.8) becomes

$$\left[M_{ij}^{e}\right]=\begin{bmatrix}0&0&0&0&0&0&0&0&0\\0&0&0&0&0&0&0&0&0\\0&0&0&0&0&0&0&0&0\\0&0&0&0&0&0&0&0&0\\0&0&0&0&0&0&0&0&0\\0&0&0&0&0&0&0&0&0\\0&0&0&0&0&0&0&0&0\\0&0&0&0&0&0&0&0&0\\0&0&0&0&0&0&0&0&0\end{bmatrix} \qquad (3.9)$$

Substituting equation (3.9) into (3.8) gives

$$\begin{bmatrix}2.785&1.201&-0.650&0&0&0&0&0&0\\1.201&10.940&1.201&0&0&0&0&0&0\\-0.650&1.201&5.570&1.201&-0.650&0&0&0&0\\0&0&1.201&10.940&1.201&0&0&0&0\\0&0&-0.650&1.201&5.570&1.201&-0.650&0&0\\0&0&0&0&1.201&10.940&1.201&0&0\\0&0&0&0&-0.650&1.201&5.570&1.201&-0.650\\0&0&0&0&0&0&1.201&10.940&1.201\\0&0&0&0&0&0&-0.650&1.201&2.785\end{bmatrix}\begin{bmatrix}T_{p2}\\T_{p3}\\T_{p4}\\T_{p5}\\T_{p6}\\T_{p7}\\T_{p8}\\T_{p9}\end{bmatrix}=800.2\begin{bmatrix}1\\4\\2\\5\\2\\5\\2\\4\\1\end{bmatrix}+\begin{bmatrix}Q_1\\0\\0\\0\\0\\0\\0\\0\\Q_9\end{bmatrix} \qquad (3.10)$$

Since $T_{p_1}=60.020^{o}F$ equation (310) condensed to becomes:

$$\begin{bmatrix}10.940&1.201&0&0&0&0&0&0\\1.201&5.570&1.201&-0.650&0&0&0&0\\0&1.201&10.940&1.201&0&0&0&0\\0&-0.650&1.201&5.570&1.201&-0.650&0&0\\0&0&0&1.201&10.940&1.201&0&0\\0&0&0&-0.650&1.201&5.570&1.201&-0.650\\0&0&0&0&0&1.201&10.940&1.201\\0&0&0&0&0&-0.650&1.201&2.785\end{bmatrix}\begin{bmatrix}Tp_2\\Tp_3\\Tp_4\\Tp_5\\Tp_6\\Tp_7\\Tp_8\\Tp_9\end{bmatrix}=\begin{Bmatrix}3200.8\\1600.4\\4001.0\\1600.4\\4001.0\\1600.4\\3200.8\\1600.4\end{Bmatrix}\begin{bmatrix}0\\0\\0\\0\\0\\0\\0\\Q_9\end{bmatrix} \qquad (3.11)$$

Since there are now eight unknown,

$$[K_{ij}]\{T_p\}=\{F_{ij}^{e}\}+\{Q_{ij}^{e}\}$$
$$[T_p]=[K_{ij}]^{-1}\{F_{ij}^{e}\}+\{Q_{ij}^{e}\}$$
$$Tp_1=60.02$$
$$Tp_2=277.20$$
$$Tp_3=140.50$$
$$Tp_4=359.32$$
$$Tp_5=-82.20$$
$$Tp_6=350.59$$
$$Tp_7=220.01$$
$$Tp_8=209.18$$
$$Tp_9=539.67$$

$\therefore Tp_1$ =60.02^{oF}, Tp_2 = 277.20^{oF}, Tp_3 =140.50^{oF}, Tp_4 = 359.32^{oF}, Tp_5 =-82.20^{oF}, Tp_6 = 350.59^{oF}, Tp_7 =220.01^{oF}, Tp_8 =209.10^{Of}, Tp_9 = 539.67^{oF}.

4.0 Exact solution

Recall equation (2.1)

$$\alpha\beta\frac{d^2T_p}{dx^2}+\beta\frac{dT_p}{dx}-T_p+T_{Fs}+g_G \qquad (4.1)$$

$$Tp(x)=C_1\ell^{y_1x}+C_2\ell^{y_2x}+g_{Gx}+T_{Fs}-\beta g_G \qquad (4.2)$$

Where

$$y_1=\frac{\beta+\sqrt{\beta^2+4\alpha\beta}}{2\alpha\beta} \qquad (4.3)$$

$$y_2 = \frac{\beta - \sqrt{\beta^2 + 4\alpha\beta}}{2\alpha\beta} \quad (4.4)$$

Substituting values of α, β into equation (4.3) and (4.4) gives

$$y_1 = 1.477,\ y_2 = -0.677$$

From equation (4.2)

$$\frac{dTp}{dx} = y_1 C_1 \ell^{y_1} + y_2 C_2 \ell^{y_2 x} + g_G \quad (4.5)$$

At $X = 0, \quad Tp(x) = Tp_j$

$X = h',\ Tp(x) = T_{Fs}(x)$

Where

Tp_s = fluid temperature at drill pipe in let or at the surface (^oF)

h' = the total vertical depth of the well (ft)

Applying the boundary conditions, the following expressions were obtained for the constants C_1 and C_2 as:

$$C_1 = \frac{g_G - \ell_{y_2}^{y_2 h'} Tdiff}{\ell_{y_2}^{y_2 h'} - \ell_{y_1}^{y_1 h'}} \quad (4.6)$$

$$C_2 = \frac{g_G - \ell_{y_1}^{y_2 h'} Tdiff}{\ell_{y_2}^{y_2 h'} - \ell_{y_1}^{y_1 h'}} \quad (4.7)$$

Where

$$Tdiff = \left(T_{Fs} - T_{ps} - Bg_G\right)$$

Substituting equations (4.6) and (4.7) into equation (4.2) gives

$$T_{p(x)} = \frac{g_G - \ell_{y_2}^{-0.677 h'} Tdiff}{\ell_{y_2}^{-0.677 h'} - \ell_{y_1}^{1.477 h'}} \ell^{1.477} + \frac{-g_G + \ell_{y_1}^{1.477 h'} Tdiff}{\ell_{y_2}^{-0.677 h'} - \ell_{y_1}^{1.477 h'}} \ell^{-0.677} + g_G + T_{Fs} - \beta g_G \quad (4.8)$$

5.0 Results and Discussion

The temperature distribution at nodes for difference meshes using quadratic interpolation functions are shown in Table 5.1. The numerical values of the calculated nodal degree of freedom shows temperature variation in the wellbore. Figure 5.1shows the results obtained using the quadratic element and the exact, it can be seen that within the range of 2.0, -1.5, 3.4, there is a marked difference between the solutions obtained using the analytical and quadratic finite element solution. The reason for this deviation is as a result of the fact that the gradient of solution within these ranges is very high. It can be seen that the finite element solution is admirably close to the exact at all points along the domain.

Table 5.1: Showing nodal temperature distribution along wellbore for quadratic interpolation and exact solution

Depth (ft)	**Nodal temperature for quadratic elements (^oF)**	**Exact nodal temperature (^oF)**
0	60.02	60.00
10	277.20	279.20
20	140.50	141.00
30	359.32	360.20
40	-82.20	-83.10
50	350.59	360.20
60	220.01	221.10
70	209.18	210.20
80	539.67	540.15

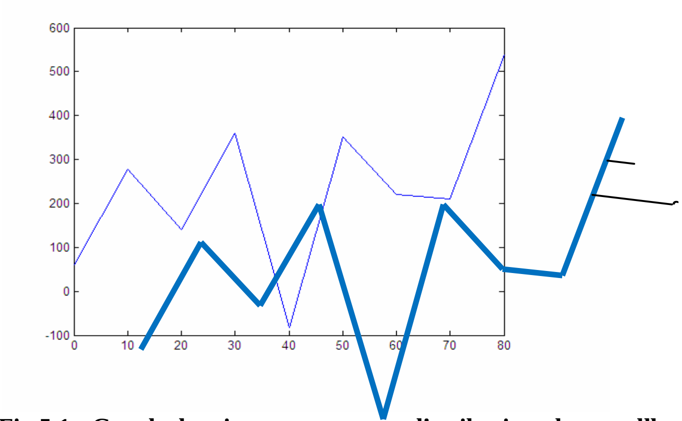

Fig 5.1: Graph showing temperature, distribution along wellbore during drilling operation

6.0 Conclusion

Finite element analysis of the temperature distribution in wellbore during drilling operation has been presented. It has be shown that the present method can be used to predict the temperature distribution accurately with mesh refinement. The finite element method has been shown to produce an accurate solution to the equations governing the temperature distribution in wellbore during drilling operation. The potential of the finite element method has been successfully demonstrated.

References

[1] Arnold, F.C. (1990): Temperature variation in circulating wellbore fluid. Journal of Energy Resources. Vol. 112, pp.79-83

[2] Beirute, R.M. (1991): A circulating and shut-in well temperature profile simulator. Journal of Petroleum Technology. Issue 9, pp.1140 – 1146

[3] Garcia, A, Santoyo, E, Espinosa, G and Hernande Z,I (1998): Estimation of Temperatures in geothermal wells during circulation and shut-in in presence of loss circulation transport in porous media. Journal of Petroleum Technology. Vol. 33, pp.103-127

[4] Ramey, H.J. (1962): "Wellbore Heat Transmission". Journal of Petroleum Technology. Pp. 427-35.

[5] Raymond, L.R (1969): Temperature distribution in a circulating drilling fluid. Journal of Petroleum Technology. Vol. 21. pp333-341.

[6] Rommetveit, R. and Bjorkevoll, K.S. (1997): Temperature and pressure, effects on drilling fluid theology and ECD in vary Deep Wells. SPE39282, Bahrain, 23-25.

[7] Takahashi, W., Osato, K, Takasugi, S and White S.P. (1997) Estimation of Formation Temperature from inlet and outlet mud temperature while drilling proceedings. 22nd Workshop on Geothermal Reservoir Engineering, StanfordUniversity, Stanford, CA, 279 – 286

[8] Tragasser, A.F., Crawford, P.B., and Horace, R.A. (1967): A method for calculating circulating temperature. Journal of Petroleum Technology. Vol. 19, pp1507-1512

[9] Wooley, G.R. (1980): Computing downhole temperatures in circulation injection and production wells. Journal of Petroleum Technology, September, 1509-1522